Regenerative Therapy 26 (2024) 547–556

Contents lists available at ScienceDirect

Regenerative Therapy

journal homepage: http://www.elsevier.com/locate/reth

Original Article

Wharton's jelly stem cells delivered via a curcumin-loaded nanofibrous wound dressings improved diabetic wound healing via upregulating VEGF and IGF genes: An in vitro and in vivo study

Chengjin Chen [a, 1], Hui Zhao [a, 1], Wenlu Zhang [b], Xuelan Hong [a, **], Shengjie Li [a, *], Saeed Rohani [c]

[a] Department of Orthopedics and Traumatology, The Third People's Hospital of Yunnan Province, Kunming City, 650000, China
[b] Rehabilitation Medicine Department, The Third People's Hospital of Yunnan Province, Kunming City, 650000, China
[c] Department of Tissue Engineering and Applied Cell Science, Tehran University of Medical Sciences, Tehran, 444522125, Iran

ARTICLE INFO

Article history:
Received 13 May 2024
Received in revised form
15 June 2024
Accepted 27 June 2024

Keywords:
Diabetic wounds
Endocrine system
Wound healing
Nanofibers
Wound dressing

ABSTRACT

Diabetic wounds pose an enduring clinical hurdle, marked by delayed recovery, persistent inflammation, and an elevated susceptibility to infections. Conventional treatment approaches often fall short of delivering optimal outcomes, prompting the exploration of innovative methods to enhance the healing process. Electrospun wound dressings offer superior healing, controlled drug release, enhanced cell proliferation, biocompatibility, high surface area, and antimicrobial properties. In the current study, polycaprolactone/gelatin-based nanofibrous wound dressings were developed for the delivery of Wharton's jelly stem cells and curcumin into the diabetic wounds bed. Curcumin was loaded into the polycaprolactone/gelatin solution and electrospun to produce curcumin-loaded scaffolds. In vitro experiments including scanning electron microscopy, cell viability assay, release assay, hemocompatibility assay, cell proliferation assay, and antibacterial assay were utilized to characterize the delivery system. Then, curcumin-loaded scaffolds were seeded with 30,000 Wharton's jelly stem cells and implanted into a rat model of diabetic wounds. Study showed that the scaffolds containing both Wharton's jelly stem cells and curcumin significantly improved diabetic wound closure (86.32 3.88% at the end of 14th day), augmented collagen deposition, and improved epithelial tissue formation. Gene expression studies showed that VEGF and IGF genes were significantly upregulated by the co-delivery system. Our developed system may have augmented diabetic wound healing via upregulating pro-healing genes.

1. Introduction

Diabetic wounds pose an enduring clinical hurdle, marked by delayed recovery, persistent inflammation, and an elevated susceptibility to infections. Conventional treatment approaches often fall short of delivering optimal outcomes, prompting the exploration of innovative methods to enhance the healing process [1–3]. This investigation introduces an inventive therapeutic strategy that combines Wharton's Jelly stem cells (WJSCs) with electrospun polycaprolactone/gelatin wound dressings loaded with curcumin to address the intricate pathophysiology of diabetic wounds.

Wharton's Jelly, a gelatinous substance found in the umbilical cord, has emerged as a valuable source of mesenchymal stem cells known for their distinctive immunomodulatory and regenerative properties [4–6]. Although these cells exhibit promise in various therapeutic applications, their potential is frequently hindered by challenges associated with efficient delivery to the wound site [7,8]. In response to this limitation, our study explores the utilization of electrospun polycaprolactone/gelatin wound dressings as a medium for the controlled release of Wharton's Jelly stem cells, with the aim of maximizing their therapeutic potential in the microenvironment of diabetic wounds.

* Corresponding author.
** Corresponding author.
E-mail addresses: 13211670682m@sina.cn (X. Hong), mayaherui1@sina.com (S. Li).

Peer review under responsibility of the Japanese Society for Regenerative Medicine.

[1] These authors contributed equally to this work.

https://doi.org/10.1016/j.reth.2024.06.018

Curcumin, a polyphenolic compound derived from turmeric, has demonstrated noteworthy anti-inflammatory, antioxidant, and wound healing properties [9]. In diabetic wounds, where healing is impeded by oxidative stress and chronic inflammation, the incorporation of curcumin into the dressing adds an extra layer of therapeutic benefit [10–12]. The controlled release of curcumin from the polycaprolacton/gelatin matrix complements the regenerative capabilities of WJSCs, producing a synergistic effect that addresses various aspects of diabetic wound pathophysiology.

The electrospinning technique employed in the production of polycaprolactone/gelatin wound dressings enables the creation of nanofibrous structures that mimic the extracellular matrix of native tissue [13,14]. This distinctive architecture enhances cell adhesion, proliferation, and migration, establishing an optimal microenvironment for the administered WJSCs [15]. Moreover, the nanofibrous structure facilitates the sustained release of curcumin, ensuring prolonged exposure to its therapeutic effects at the wound site. Yang et al. showed that electrospun silk fibroin scaffolds serve as an effective delivery system for mesenchymal stem cells (MSCs) to treat diabetic wounds [16]. Golchin et al. utilized chitosan/polyvinyl alcohol/carbopol/polycaprolactone nanofibers loaded with curcumin for the local delivery of MSCs in wound healing applications [17].

This investigation builds upon prior studies illustrating the effectiveness of stem cell-based therapies and curcumin in diabetic wound healing. However, the integration of WJSCs within electrospun polycaprolactone/gelatin dressings, coupled with the controlled release of curcumin, presents a groundbreaking and comprehensive approach to address the multifaceted challenges posed by diabetic wounds. By concentrating on both the cellular and molecular aspects of wound healing, this study aims to assess the healing potential of this system in a rat model of diabetic wound healing. This is the first study developing a delivery system for WJSCs and curcumin for wound healing applications.

2. Methods and materials

2.1. Preparation of curcumin-loaded polycaprolactone/gelatin nanofibers

Gelatin of Type A (purchased from Sigma Aldrich) and polycaprolactone (PCL) were dissolved in acetic acid (Glacial, procured from Merck) at 90:10 wt ratio and at final concentration of 14 wt% over a duration of 12 h. Subsequently, curcumin powder, obtained from Sigma Aldrich, was introduced to the polymeric solution at a weight ratio of 2 w/w% and thoroughly mixed for 6 h. The resulting solution was then loaded into a 10 ml disposable syringe and subjected to the electrospinning process under specific conditions, including a positive high voltage of 18 kV, a feeding rate of 1 ml/h, a needle-to-collector distance of 17 cm, and a collector turning rate ranging between 500 and 600 rpm.

2.2. MTT assay

The assessment of L929 fibroblast cell viability cultured on the engineered scaffolds took place on days 1, 3, and 5 using the MTT (3-(4,5-dimethylthiazol-2-yl)-2,5-diphenyltetrazolium bromide) assay. At each specified time point, the scaffolds hosting the cell population (7000 cells per scaffold) were delicately retrieved from the culture plates. Before conducting the viability assessment, the scaffolds underwent a gentle cleansing with phosphate-buffered saline (PBS) to eliminate non-adherent cells and any extraneous debris. This step ensured that subsequent viability measurements accurately reflected the cells firmly attached to the scaffold surfaces. The MTT assay involved adding a solution of MTT reagent (0.5 mg/ml) to each well containing the cell-seeded scaffolds. After an incubation period of 4 h at 37 °C, formazan crystals produced by metabolically active cells were dissolved using dimethyl sulfoxide (DMSO). Subsequently, the spectrophotometric measurement of the resulting solution's absorbance was conducted at a wavelength of 570 nm. Curcumin-loaded and curcumin-free scaffolds were named CURPCLGEL and PCLGEL scaffolds, respectively.

2.3. MTT assay under oxidative stress

L929 cells were placed on the sterilized scaffolds at a density of 7000 cells per scaffold and cultivated for 48 h. Subsequently, the culture medium was enriched with 1% H2O2, and the cells were incubated for a duration of 1 h. Finally, a cell viability assay was conducted following the previously outlined procedure.

2.4. Release assay

The evaluation of curcumin release from CURPCLGEL scaffolds was conducted using PBS as the release medium. To summarize, 100 mg of the electrospun scaffolds was immersed in 20 ml of PBS for a duration of 7 days. At various time intervals, a small sample of the release medium was extracted, and its absorbance was measured at 420 nm. The obtained values were then incorporated into the curcumin standard curve, enabling the calculation of cumulative drug release over time.

2.5. DPPH assay

The radical scavenging capability of CURPCLGEL scaffolds was assessed using DPPH assay method as described before [18].

2.6. Bacterial penetration assay

Bacterial penetration assay was performed according to a method as described before [19]. Customizing the method for CURPCLGEL and PCLGEL scaffolds, the microbial penetration test evaluated the effectiveness of the dressings in preventing microbial intrusion. Specifically, 10 ml vials with a test area of 0.8 cm^2, containing 5 ml of BHI broth culture medium, were sealed with the prepared counterparts of CURPCLGEL and PCLGEL scaffolds. These vials were then placed under ambient conditions, and the degree of bacterial penetration into the culture medium was measured after 3 and 7 days. Negative controls involved bottles covered with a cotton ball, while open vials served as positive controls. The turbidity, indicative of microbial contamination, was quantified through spectroscopy at 600 nm using a microplate spectrophotometer.

2.7. Water vapor permeation test

Permeability of CURPCLGEL and PCLGEL scaffolds to gases was assessed using a water vapor permeability test as described before [19]. In brief, square-shaped scaffolds were cut and employed to cover bottles with an opening surface area of 1.3 cm^2, which have been filled with 5 ml of distilled water. These bottles were then placed at 37 °C for 24 h. Finally, the assessment of water vapor permeation through the scaffolds was conducted using the following formula:

$$\text{Water vapor permeation} = \frac{\textit{Water weight loss}}{\textit{Surface area} \times \textit{time}}$$

2.8. Mechanical strength studies

The assessment of the ultimate tensile strength for CURPCLGEL and PCLGEL scaffolds (4.5 × 1.7 cm^2 pieces with the thickness of around 350 μm) was conducted through a uniaxial tensile testing apparatus, employing an extension rate of 1 mm/min.

2.9. Preparation of WJSCs-seeded scaffolds for implantation

The sterilization of CURPCLGEL and PCLGEL scaffolds involved a 1-h treatment with 70% ethanol, followed by multiple rinses using DMEM culture media repeated five times. Subsequently, the scaffolds were seeded with WJSCs (ATCC, USA) at a density of 30,000 cells/cm^2 and cultured for 48 h in DMEM culture media (Invitrogen) supplemented with 10 v/v% FBS and 1% antibiotics (Gibco). On the day of implantation, the scaffolds were withdrawn from the culture media and positioned onto the wound area.

2.10. In vivo study

All animal experiments were conducted in accordance with the U.K. Animals (Scientific Procedures) Act, 1986 and associated guidelines, the European Communities Council Directive of November 24, 1986 (86/609/EEC) or the National Institutes of Health guide for the care and use of Laboratory animals (NIH Publications No. 8023, revised 1978). Male Wistar rats (weighing 200–250 g) were induced into diabetes through intraperitoneal injection of Streptozotocin (60 mg/kg). The criterion for diabetes induction was a fasting blood sugar level above 250 mg/dl. Twelve diabetic rats were randomly allocated into four groups, each comprising three animals: 1) WJSCs-seeded CURPCLGEL scaffolds (WJSCs-CURPCLGEL group), 2) WJSCs-seeded PCLGEL scaffolds (WJSCs-PCLGEL group), 3) Negative control group (no treatment applied after injury), and 4) Positive control group (treated with commercially available wound dressing, Medihoney® wound gel).

The surgical procedure commenced with intraperitoneal injection of Ketamine 5%/Xylazine 2% (70 mg ketamine and 6 mg xylazine per 1 kg body weight). Subsequently, the dorsum skin of the animals was sheared, disinfected, and a 1.5 cm diameter square full-thickness wound was created. The dressings were then applied to the wound area and secured in place with adhesive bandages. On days 7 and 14, the macroscopic appearance of the wounds was evaluated, and wound sizes were measured using a digital caliper. Finally, on the 14th day, the animals were euthanized, and wound tissues were collected for histopathological examination using H&E and Masson's trichrome staining. The percentage of wound closure and epithelium thickness were calculated based on images from each respective group.

2.11. Gene expression studies

Relative mRNA expression of VEGF and IGF genes was assessed using real time PCR assay on day 14th after the injury. Briefly, the extraction of total RNA from wound tissue samples was conducted utilizing an RNA extraction kit (Denazist, Iran) following the manufacturer's provided protocol. The synthesis of cDNA templates was carried out using a cDNA Reverse Transcription Kit (Denazist, Iran) in accordance with the manufacturer's instructions. Gene amplification involved 20 μl of reaction master mix containing Power SYBR Green, cDNA, and primers. The GAPDH gene served as the housekeeping gene, and the $2-\Delta\Delta ct$ method was employed to calculate the relative gene expression profile. Primers for various genes are detailed in Table 1.

Table 1
Primer sequences used in the real time PCR assay.

Gene	Forward (5′–3′)	Reverse (5′–3′)
VEGF	GACTGGAAGCTGTGGAGATGCA	GGCTGCACTGAGTTCTTTGCCA
IGF	CTCTTCAGTTCGTGTGTGGAGAC	CAGCCTCCTTAGATCACAGCTC
GAPDH	GGGAAACTGTGGCGTGAT	AAAGGTGGAGGAGTGGGT

2.12. Statistical analysis

Statistical analysis of the data was performed using GraphPad Prism, employing both student's t-test and one-way ANOVA. All experiments were repeated at least three times.

3. Results

3.1. SEM imaging results

The findings from Fig. 1 demonstrated that both CUPCLGEL and PCLGEL scaffolds exhibited a high level of porosity, characterized by fibers arranged in a random orientation. These fibers appeared smooth, and their size distribution was relatively broad. According to size measurements, the CUPCLGEL and PCLGEL scaffolds had dimensions of approximately 452.72 ± 223.88 nm and 515.94 ± 236.86 nm, respectively.

3.2. Cell viability assay results

The outcomes of the MTT assay (depicted in Fig. 2 A) indicated that under normal conditions, both CUPCLGEL and PCLGEL scaffolds did not induce notable toxicity in L929 cells. Nevertheless, when exposed to oxidative stress, cells cultured on tissue culture plates and PCLGEL scaffolds exhibited significantly reduced cell viability compared to those cultured on CUPCLGEL scaffolds (Fig. 2 B).

3.3. Release assay results

The findings from Fig. 3 A revealed a gradual release of curcumin from the matrix of CUPCLGLE scaffolds. Initially, the drug release exhibited a relatively faster pace, which subsequently decelerated. By the end of the 7th day, the rate of curcumin release had reached to 61.97 ± 3.52 %.

3.4. DPPH assay results

The findings from Fig. 3 B indicated that the radical scavenging activity of CUPCLGEL scaffolds was notably greater than that of PCLGEL scaffolds. Nevertheless, across all concentrations, the ascorbic acid group exhibited significantly higher radical scavenging activity compared to the other groups.

3.5. Bacterial penetration assay

The outcomes depicted in Fig. 3C revealed that the turbidity of BHI media in bottles sealed with CUPLCGEL scaffolds was markedly lower compared to the other groups. There were no significant differences between the PCLGEL and cotton ball groups. Notably, open bottles exhibited significantly higher turbidity than the other groups.

3.6. Water vapor permeation test results

Results showed that PCLGEL and CUPCLGEL wound dressings allowed significant amount of water vapor to pass through them.

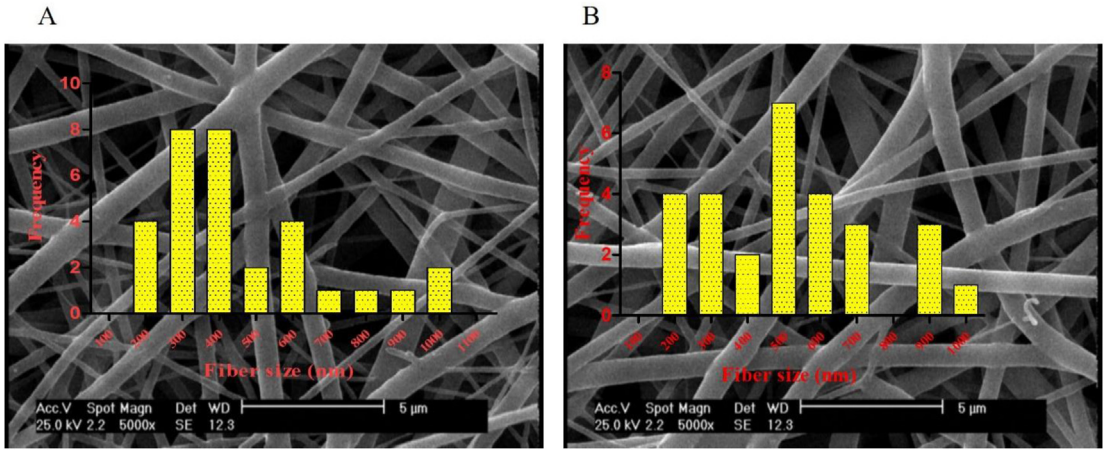

Fig. 1. SEM images (A) CUPCLGEL and (B) PCLGEL scaffolds.

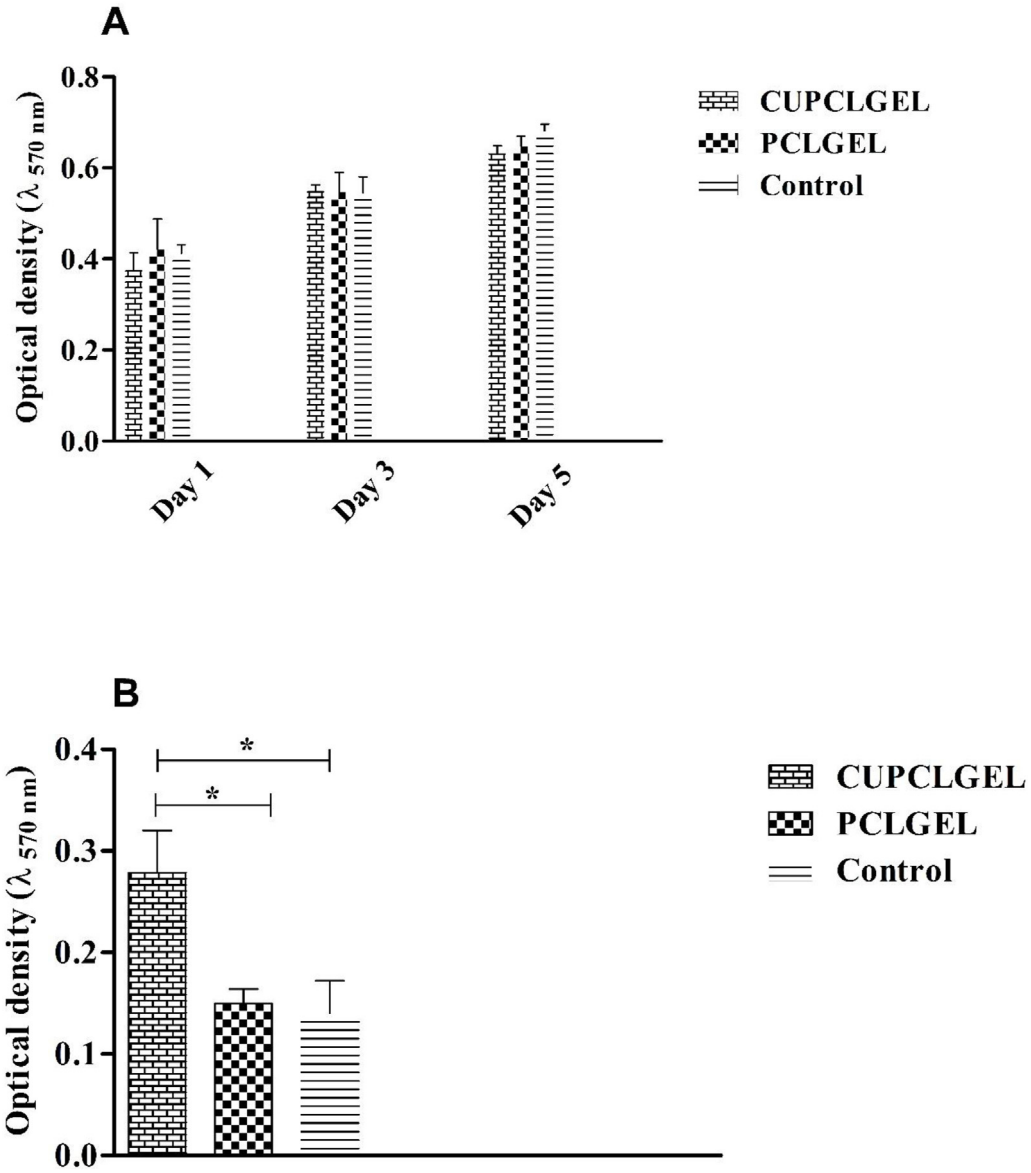

Fig. 2. Cell viability assay (A) without oxidative stress and (B) with oxidative stress, * shows p-value <0.05.

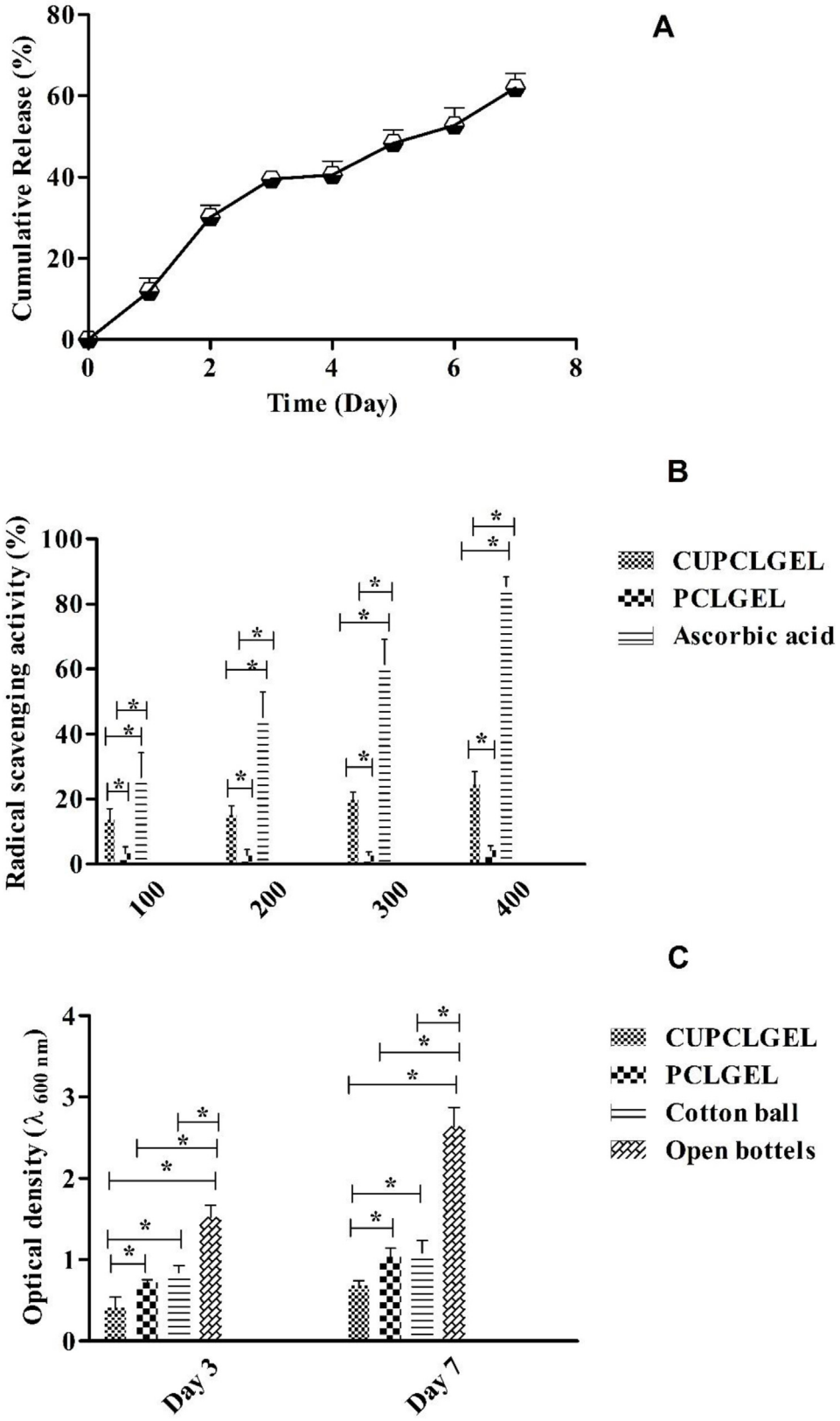

Fig. 3. (A) shows the release of curcumin from the matrix of CUPCLGEL scaffolds, (B) shows results of DPPH assay, and (C) shows bacterial penetration assay results, * shows p-value <0.05.

The amount of water vapor permeation for CUPCLGEL and PCLGEL scaffolds was measured to be around 126.76 ± 22.05 mg h^{-1} cm^{-2} and 138.58 ± 5.60 mg h^{-1} cm^{-2}, respectively. Differences between groups were not significant.

3.7. Mechanical strength analysis results

Our study showed that CUPCLGEL and PCLGEL scaffolds had around 3.03 ± 0.36 MPa and 3.22 ± 0.25 MPa of ultimate tensile strength, respectively. Differences were not significant.

3.8. In vivo study

Results (Figs. 4 and 5 A) showed that on day 14th, percentage of wound closure in the positive control group was significantly higher than other groups. On the same time step, the animals treated with WJSCs-CURPCLGEL group had significantly higher percentage of wound closure than WJSCs-PCLGEL and negative control groups. In addition, WJSCs-PCLGEL group had significantly higher percentage of wound closure than the negative control group. Histopathological studies (Fig. 6) showed that the positive control group exhibited advanced wound repair, characterized by well-organized tissue architecture, increased cellular density, reduced inflammation, and extensive collagen fiber maturation. The WJSCs-CURPCLGEL group demonstrated enhanced tissue regeneration compared to the negative control, with notable cellular proliferation and reduced inflammation. Masson's trichrome staining indicated increased collagen deposition, though slightly less mature than the positive control. The WJSCs-PCLGEL group exhibited moderate tissue regeneration, with evidence of cellular activity and reduced inflammation. Collagen deposition, while present, appeared less mature than both positive control and WJSCs-CURPCLGEL groups. The negative control group displayed poor tissue regeneration, minimal cellular proliferation, persistent inflammation, and disorganized collagen fibers. These findings underscore the positive impact of the wound dressings, particularly WJSCs-CURPCLGEL, on the histological parameters associated with wound healing, providing valuable insights for potential clinical applications. Histomorphometry analysis (Fig. 5 B and C) showed that percentage of wound closure and thickness of epithelium in the WJSCs-CURPCLGEL group were significantly higher than negative control and WJSCs-PCLGEL groups. These values for the positive control group were significantly higher than other groups.

3.9. Gene expression studies

Results (Fig. 7) showed that the relative mRNA expression of VEGF and IGF genes in the positive control and WJSCs-CURPCLGEL groups was significantly higher than WJSCs-PCLGEL group.

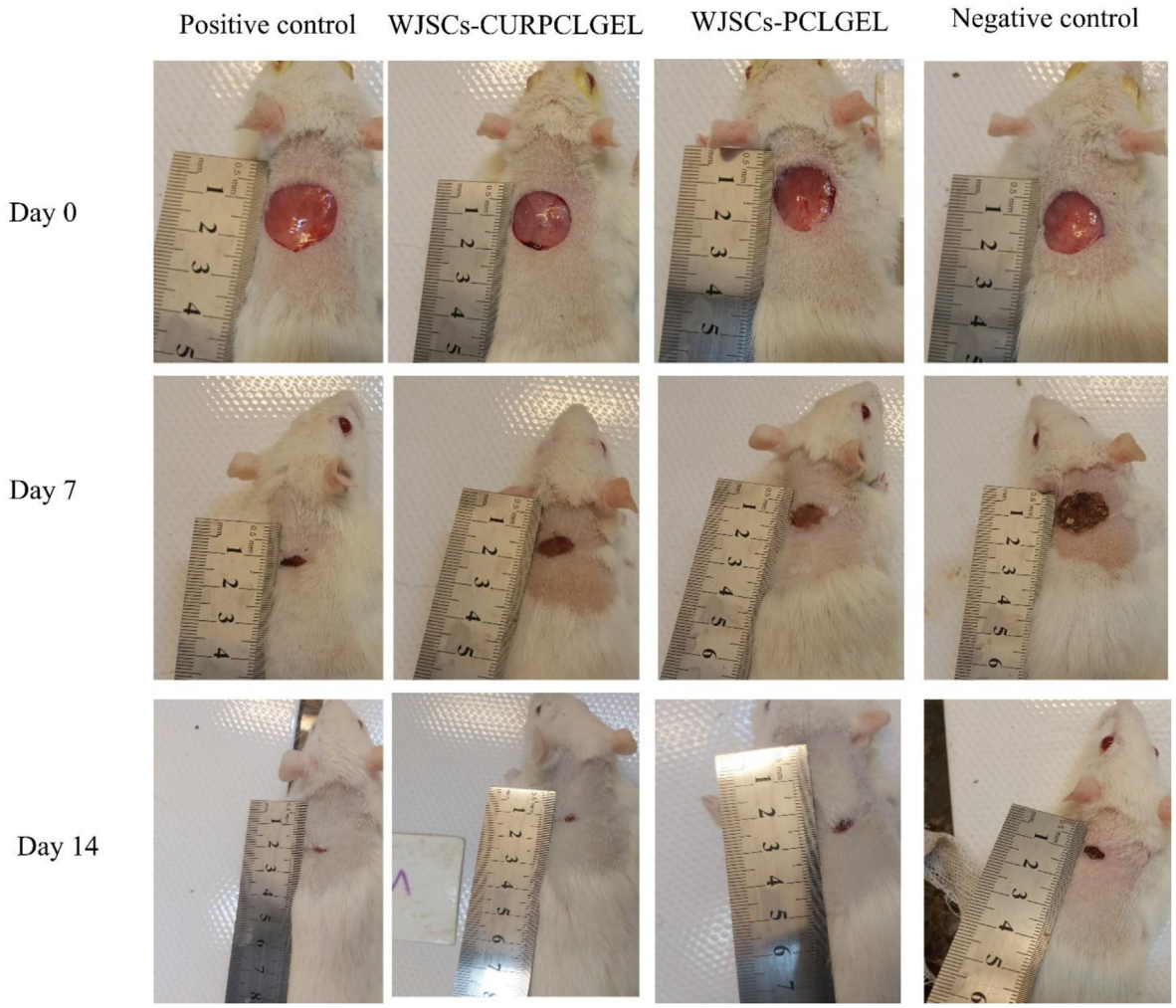

Fig. 4. In vivo wound closure assay in animals treated with different dressings on days 7 and 14 after wounding.

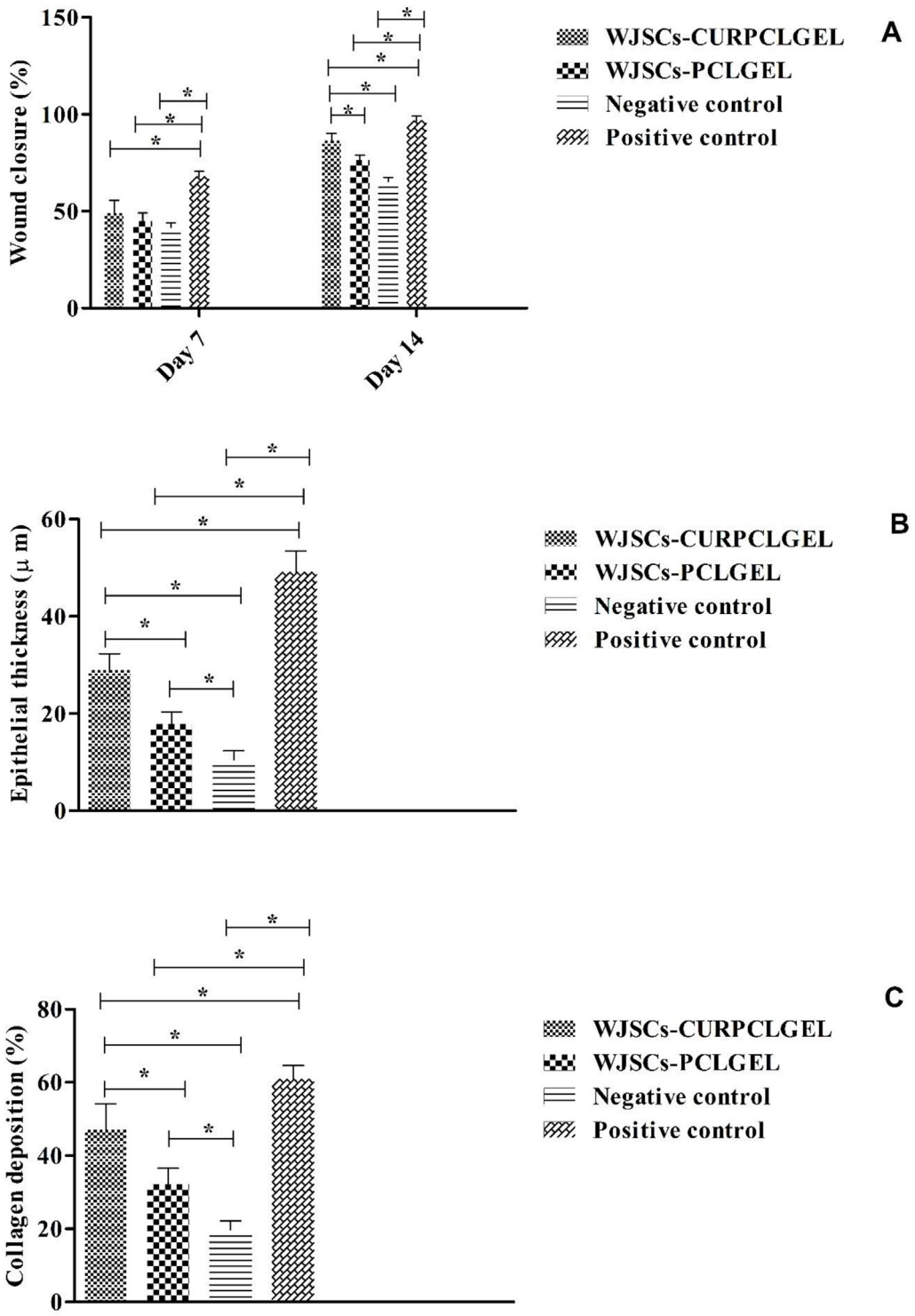

Fig. 5. Histograms comparing (A) percentage of wound size reduction, (B) epithelium thickness, and (C) collagen deposition in wounds treated with different dressings, * shows p-value <0.05.

Differences between the positive control and WJSCs-CURPCLGEL groups were not significant.

4. Discussion

Electrospun wound dressings integrate cell and drug delivery, representing an advanced approach to wound care. These nanofibrous structures, fabricated through electrospinning, offer a unique platform for simultaneously administering therapeutic cells and drugs directly to the wound site [20–23]. The high surface area of the electrospun matrix supports cell adhesion and proliferation, fostering accelerated tissue regeneration [24–26]. Controlled release of bioactive compounds enhances wound healing by reducing inflammation and promoting cellular activities. In our

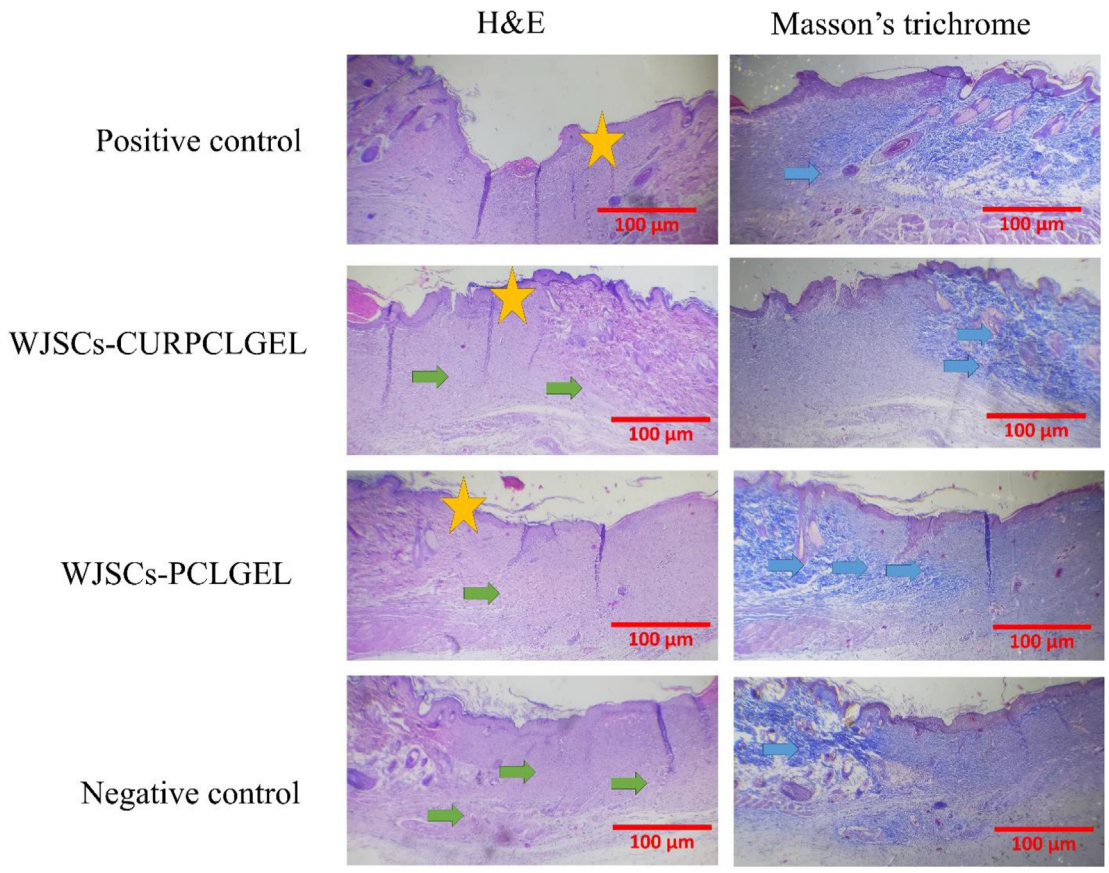

Fig. 6. Histopathological staining images of wounds treated with different dressings stained with H&E and Masson's trichrome.

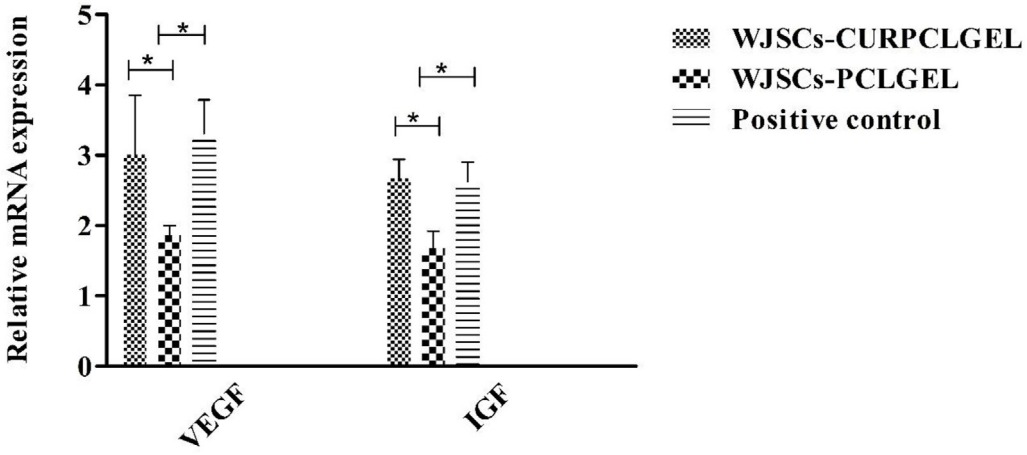

Fig. 7. Relative mRNA expression of VEGF and IGF genes in wounds treated with different dressings on day 14th of wounding, * shows p-value <0.05.

current research, we developed a delivery system for both curcumin and WJSCs in order to augment diabetic wound healing. The microstructure of our developed delivery system resembled native skin tissue's ECM. This similarity suggests that our system may effectively mimic the natural environment, potentially enhancing compatibility for WJSCs and promoting favorable interactions for targeted cell and drug delivery, thus optimizing therapeutic outcomes [21,22,27]. In accordance with the results of previous studies, we could show the biocompatibility of our scaffolds. Under oxidative stress, CUPCLGEL scaffolds had significantly higher cell viability than other groups. This result can be attributed to the presence of curcumin in the matrix of electrospun scaffolds [28,29]. This drug shields cells from oxidative stress by exerting potent antioxidant effects. It effectively scavenges various reactive oxygen species, including superoxide anion radicals, hydroxyl radicals, and nitrogen dioxide radicals, while promoting the synthesis of antioxidant enzymes such as SOD, CAT, and GPx. Additionally, curcumin activates the Nrf2-Keap1 pathway, enhancing the activity of antioxidant enzymes and further contributing to its ability to mitigate oxidative stress. Furthermore, curcumin's capacity to penetrate

mitochondria plays a crucial role in protecting retinal neuronal cells from oxidative damage and preventing mitochondrial dysfunction induced by oxidative stress [30–33]. This theory was validated by the results of DPPH assay that showed that incorporation of curcumin into the electrospun scaffolds significantly augmented their radical scavenging activity. Curcumin exhibits the capability to neutralize free radicals through the resonance stabilization of its radicals, primarily derived from the two phenolic OH groups or the CH2 group within the β-diketone moiety. This function stems from the compound's capacity for “electron transfer” and/or “H-atom donation,” allowing it to effectively engage with and counteract free radicals [34]. The prolonged release pattern of curcumin from the scaffolds may result from factors such as diffusion, the expansion of the PCL/gelatin structure, and biodegradation [35–37]. Bacterial penetration assay showed that CUPCLGEL scaffolds could deficiently block the invasion of bacteria through the scaffolds. This result could be attributed to the antibacterial activity of curcumin. This agent causes disturbance to the bacterial membrane, hinders the generation of bacterial virulence factors, and disrupts the bacterial quorum sensing regulation system. Research has additionally indicated that the antibacterial effectiveness of curcumin is specifically associated with its methoxy and hydroxy derivatives [38–40]. The excellent water vapor permeability of CUPCLGEL scaffolds guarantees the passage of oxygen, preventing any risk of wound maceration [41]. This property can be attributed to the porous microarchitecture of scaffolds. The elevated tensile characteristics of our delivery system can be attributed to the significant presence of PCL within the scaffolds' matrix [42,43]. The in vivo examination demonstrated a notably superior wound healing capacity in WJSCs-CURPCLGEL dressings compared to both WJSCs-PCLGEL and negative control groups. This positive therapeutic effect was concomitant with an increase in the expression of VEGF and IGF genes. It appears that the collaborative healing properties of curcumin and WJSCs are responsible for this enhanced wound healing capability. Curcumin's wound healing prowess stems from its anti-inflammatory, antioxidant, and antimicrobial attributes found in turmeric. Zhang et al. showed that the therapeutic effect of curcumin on wound healing is enhanced by the overexpression of TRPM7, which operates through the STAT3/SMAD3 signaling pathway in human fibroblasts [44]. Curcumin supports the various phases of wound recovery by reducing inflammation, preventing infections, and promoting growth factors like VEGF and IGF [10,11,45–47]. In addition, WJSCs possess anti-inflammatory attributes, mitigating excessive immune responses and creating an optimal setting for repair. Through their promotion of angiogenesis, WJSCs facilitate the formation of new blood vessels, ensuring improved nutrient and oxygen supply to the wounded area. Additionally, their paracrine signaling influences neighboring cells, orchestrating a synchronized response [48–52]. Chen et al. analyzed analyzes WJSCs heterogeneity using single-cell and spatial transcriptomics, identifying four subpopulations. They highlighted the potential of S100A9+CD29^{+}CD142+ cells from the fetal segment of the umbilical cord for wound healing therapies [53]. This study suggests potential applicability of CUPCLGEL scaffolds as a potential cell-delivery system for WJSCs in wound healing applications.

5. Conclusion

In conclusion, the integration of electrospun wound dressings, serving as a dual platform for cell and drug delivery, represents a cutting-edge approach to wound care. The developed delivery system, incorporating both curcumin and WJSCs, demonstrates promising potential for augmenting diabetic wound healing. The structural similarity of the delivery system to native skin tissue's extracellular matrix enhances compatibility for WJSCs, optimizing targeted cell and drug delivery and ultimately improving therapeutic outcomes. The biocompatibility of the scaffolds, validated under oxidative stress conditions, underscores the protective role of curcumin in shielding cells from oxidative damage. Moreover, the antibacterial properties of curcumin contribute to the scaffolds' ability to impede bacterial invasion. The study's findings highlight the enhanced wound healing capacity of WJSCs-CURPCLGEL dressings, suggesting a synergistic effect between curcumin and WJSCs. Overall, the study implies the potential clinical relevance of CUPCLGEL scaffolds as a promising cell-delivery system for advanced wound healing applications. Future research should focus on optimizing the electrospun wound dressings by refining the composition and structure to further mimic the native extracellular matrix, enhancing compatibility and therapeutic efficacy. Clinical trials will be crucial to validate the safety and effectiveness of the WJSCs-CURPCLGEL delivery system in diverse patient populations, particularly those with diabetic wounds. Investigating the long-term effects of these dressings on wound healing and their integration with other therapeutic agents could expand their applications. Additionally, exploring the scalability and cost-effectiveness of manufacturing these advanced dressings will be essential for widespread clinical adoption. The development of personalized wound care solutions, leveraging the patient's specific cellular and molecular profiles, may also emerge as a promising avenue, further advancing the field of regenerative medicine and wound management.

Funding

The authors declare that no funds, grants, or other support were received during the preparation of this manuscript.

Declaration of competing interest

None.

References

[1] Burgess JL, Wyant WA, Abdo Abujamra B, Kirsner RS, Jozic I. Diabetic wound-healing science. Medicina 2021;57(10):1072.
[2] Falanga V. Wound healing and its impairment in the diabetic foot. Lancet 2005;366(9498):1736–43.
[3] Matoori S, Veves A, Mooney DJ. Advanced bandages for diabetic wound healing. Sci Transl Med 2021;13(585):eabe4839.
[4] Davies JE, Walker JT, Keating A. Concise review: wharton's jelly: the rich, but enigmatic, source of mesenchymal stromal cells. Stem cells translational medicine 2017;6(7):1620–30.
[5] Lo Iacono M, Anzalone R, La Rocca G, Baiamonte E, Maggio A, Acuto S. Wharton's jelly mesenchymal stromal cells as a feeder layer for the ex vivo expansion of hematopoietic stem and progenitor cells: a review. Stem Cell Reviews Reports 2017;13(1):35–49.
[6] G Jeschke M, Gauglitz GG, Herndon DN, Phan TT, Kita K. Umbilical cord lining membrane and wharton's jelly-derived mesenchymal stem cells: the similarities and differences. Open Tissue Eng Regen Med J 2011;4(1).
[7] Hsu LC, Peng BY, Chen MS, Thalib B, Ruslin M, Tung TDX, et al. The potential of the stem cells composite hydrogel wound dressings for promoting wound healing and skin regeneration: in vitro and in vivo evaluation. J Biomed Mater Res B Appl Biomater 2019;107(2):278–85.
[8] Dash BC, Xu Z, Lin L, Koo A, Ndon S, Berthiaume F, et al. Stem cells and engineered scaffolds for regenerative wound healing. Bioengineering 2018;5(1):23.
[9] Gayathri K, Bhaskaran M, Selvam C, Thilagavathi R. Nano formulation approaches for curcumin delivery-a review. J Drug Deliv Sci Technol 2023;82:104326.
[10] Akbik D, Ghadiri M, Chrzanowski W, Rohanizadeh R. Curcumin as a wound healing agent. Life Sci 2014;116(1):1–7.
[11] Fereydouni N, Darroudi M, Movaffagh J, Shahroodi A, Butler AE, Ganjali S, et al. Curcumin nanofibers for the purpose of wound healing. J Cell Physiol 2019;234(5):5537–54.
[12] Alven S, Nqoro X, Aderibigbe BA. Polymer-based materials loaded with curcumin for wound healing applications. Polymers 2020;12(10):2286.

[13] Flores-Rojas GG, Gómez-Lazaro B, López-Saucedo F, Vera-Graziano R, Bucio E, Mendizábal E. Electrospun scaffolds for tissue engineering: a review. Macromolecules (Washington, DC, U S) 2023;3(3):524–53.
[14] Sharma D, Srivastava S, Kumar S, Sharma PK, Hassani R, Dailah HG, et al. Biodegradable electrospun scaffolds as an emerging tool for skin wound regeneration: a comprehensive review. Pharmaceuticals 2023;16(2):325.
[15] Jiang X, Zeng Y-E, Li C, Wang K, Yu D-G. Enhancing diabetic wound healing: advances in electrospun scaffolds from pathogenesis to therapeutic applications. Front Bioeng Biotechnol 2024;12:1354286.
[16] Xie S-Y, Peng L-H, Shan Y-H, Niu J, Xiong J, Gao J-Q. Adult stem cells seeded on electrospinning silk fibroin nanofiberous scaffold enhance wound repair and regeneration. J Nanosci Nanotechnol 2016;16(6):5498–505.
[17] Golchin A, Hosseinzadeh S, Jouybar A, Staji M, Soleimani M, Ardeshirylajimi A, et al. Wound healing improvement by curcumin-loaded electrospun nanofibers and BFP-MSCs as a bioactive dressing. Polym Adv Technol 2020;31(7):1519–31.
[18] Ye L, Gao Z, Rohani S. Intervertebral disk regeneration in a rat model by allopurinol–loaded chitosan/alginate hydrogel. Biomolecules Biomedicine 2023;5:1563–78.
[19] Samadian H, Zamiri S, Ehterami A, Farzamfar S, Vaez A, Khastar H, et al. Electrospun cellulose acetate/gelatin nanofibrous wound dressing containing berberine for diabetic foot ulcer healing: in vitro and in vivo studies. Sci Rep 2020;10(1):8312.
[20] Afsharian YP, Rahimnejad M. Bioactive electrospun scaffolds for wound healing applications: a comprehensive review. Polym Test 2021;93:106952.
[21] Gao C, Zhang L, Wang J, Jin M, Tang Q, Chen Z, et al. Electrospun nanofibers promote wound healing: theories, techniques, and perspectives. J Mater Chem B 2021;9(14):3106–30.
[22] Memic A, Abdullah T, Mohammed HS, Joshi Navare K, Colombani T, Bencherif SA. Latest progress in electrospun nanofibers for wound healing applications. ACS Appl Bio Mater 2019;2(3):952–69.
[23] Dong Y, Zheng Y, Zhang K, Yao Y, Wang L, Li X, et al. Electrospun nanofibrous materials for wound healing. Advanced Fiber Materials 2020;2:212–27.
[24] Joseph B, Augustine R, Kalarikkal N, Thomas S, Seantier B, Grohens Y. Recent advances in electrospun polycaprolactone based scaffolds for wound healing and skin bioengineering applications. Mater Today Commun 2019;19:319–35.
[25] Palanisamy CP, Cui B, Zhang H, Gunasekaran VP, Ariyo AL, Jayaraman S, et al. A critical review on starch-based electrospun nanofibrous scaffolds for wound healing application. Int J Biol Macromol 2022;222:1852–60.
[26] Preethi GU, Unnikrishnan BS, Archana MG, Mohan D, Pillai KR, Sreelekha TT. Electrospun polysaccharide scaffolds: wound healing and stem cell differentiation. J Biomater Sci Polym Ed 2022;33(7):858–77.
[27] Chen H, Peng Y, Wu S, Tan LP. Electrospun 3D fibrous scaffolds for chronic wound repair. Materials 2016;9(4):272.
[28] Farzaei MH, Zobeiri M, Parvizi F, El-Senduny FF, Marmouzi I, Coy-Barrera E, et al. Curcumin in liver diseases: a systematic review of the cellular mechanisms of oxidative stress and clinical perspective. Nutrients 2018;10(7):855.
[29] Scapagnini G, Colombrita C, Amadio M, D'Agata V, Arcelli E, Sapienza M, et al. Curcumin activates defensive genes and protects neurons against oxidative stress. Antioxidants Redox Signal 2006;8(3–4):395–403.
[30] Sathyabhama M, Priya Dharshini LC, Karthikeyan A, Kalaiselvi S, Min T. The credible role of curcumin in oxidative stress-mediated mitochondrial dysfunction in mammals. Biomolecules 2022;12(10):1405.
[31] Lin C, Wu X. Curcumin protects trabecular meshwork cells from oxidative stress. Investigative ophthalmology visual science 2016;57(10):4327–32.
[32] Maithili Karpaga Selvi N, Sridhar MG, Swaminathan RP, Sripradha R. Curcumin attenuates oxidative stress and activation of redox-sensitive kinases in high fructose-and high-fat-fed male Wistar rats. Sci Pharm 2015;83(1):159–75.
[33] Xu D, Zhang K, Qu X-H, Wang T, Yang P, Yang Y, et al. Curcumin protects retinal neuronal cells against oxidative stress-induced damage by regulating mitochondrial dynamics. Exp Eye Res 2022;224:109239.
[34] Barzegar A, Moosavi-Movahedi AA. Intracellular ROS protection efficiency and free radical-scavenging activity of curcumin. PLoS One 2011;6(10):e26012.
[35] Calori IR, Braga G, de Jesus PdCC, Bi H, Tedesco AC, et al. Polymer scaffolds as drug delivery systems. Eur Polym J 2020;129:109621.
[36] Garg T, Singh O, Arora S, Murthy R. Scaffold: a novel carrier for cell and drug delivery. Crit Rev Ther Drug Carrier Syst 2012;29(1).
[37] Sun G, Mao JJ. Engineering dextran-based scaffolds for drug delivery and tissue repair. Nanomedicine 2012;7(11):1771–84.
[38] Zheng D, Huang C, Huang H, Zhao Y, Khan MRU, Zhao H, et al. Antibacterial mechanism of curcumin: a review. Chem Biodivers 2020;17(8):e2000171.
[39] Hussain Y, Alam W, Ullah H, Dacrema M, Daglia M, Khan H, et al. Antimicrobial potential of curcumin: therapeutic potential and challenges to clinical applications. Antibiotics 2022;11(3):322.
[40] Górski M, Niedźwiadek J, Magryś A. Antibacterial activity of curcumin–a natural phenylpropanoid dimer from the rhizomes of Curcuma longa L. and its synergy with antibiotics. Ann Agric Environ Med 2022;29(3):394.
[41] Mi FL, Wu YB, Shyu SS, Schoung JY, Huang YB, Tsai YH, et al. Control of wound infections using a bilayer chitosan wound dressing with sustainable antibiotic delivery. J Biomed Mater Res 2002;59(3):438–49.
[42] Oh G, Rho J, Lee DY, Lee M-H, Kim Y-Z. Synthesis and characterization of electrospun PU/PCL hybrid scaffolds. Macromol Res 2018;26:48–53.
[43] Jeong H, Rho J, Shin J-Y, Lee DY, Hwang T, Kim KJ. Mechanical properties and cytotoxicity of PLA/PCL films. Biomedical Engineering Letters 2018;8:267–72.
[44] Zhang H, Li H, Wang H, Lei S, Yan L. Overexpression of TRPM7 promotes the therapeutic effect of curcumin in wound healing through the STAT3/SMAD3 signaling pathway in human fibroblasts. Burns 2023;49(4):889–900.
[45] Tejada S, Manayi A, Daglia M, Nabavi S F, Sureda A, Hajheydari Z, et al. Wound healing effects of curcumin: a short review. Curr Pharmaceut Biotechnol 2016;17(11):1002–7.
[46] Mohanty C, Sahoo SK. Curcumin and its topical formulations for wound healing applications. Drug Discov Today 2017;22(10):1582–92.
[47] Chereddy KK, Coco R, Memvanga PB, Ucakar B, des Rieux A, Vandermeulen G, et al. Combined effect of PLGA and curcumin on wound healing activity. J Contr Release 2013;171(2):208–15.
[48] Arno AI, Amini-Nik S, Blit PH, Al-Shehab M, Belo C, Herer E, et al. Human Wharton's jelly mesenchymal stem cells promote skin wound healing through paracrine signaling. Stem Cell Res Ther 2014;5(1):1–13.
[49] Shohara R, Yamamoto A, Takikawa S, Iwase A, Hibi H, Kikkawa F, et al. Mesenchymal stromal cells of human umbilical cord Wharton's jelly accelerate wound healing by paracrine mechanisms. Cytotherapy 2012;14(10):1171–81.
[50] Fong CY, Tam K, Cheyyatraivendran S, Gan SU, Gauthaman K, Armugam A, et al. Human Wharton's jelly stem cells and its conditioned medium enhance healing of excisional and diabetic wounds. J Cell Biochem 2014;115(2):290–302.
[51] Himal I, Goyal U, Ta M. Evaluating Wharton's jelly-derived mesenchymal stem cell's survival, migration, and expression of wound repair markers under conditions of ischemia-like stress. Stem Cell Int 2017;2017.
[52] Arno AI, Amini-Nik S, Blit PH, Al-Shehab M, Belo C, Herer E, et al. Effect of human Wharton's jelly mesenchymal stem cell paracrine signaling on keloid fibroblasts. Stem cells translational medicine 2014;3(3):299–307.
[53] Chen P, Tang S, Li M, Wang D, Chen C, Qiu Y, et al. Single-cell and spatial transcriptomics decodes wharton's jelly-derived mesenchymal stem cells heterogeneity and a subpopulation with wound repair signatures. Adv Sci 2023;10(4):2204786.